CrossMark
click for updates

Publish Free
Access

PEGylated nanohydrogels delivering anti-MicroRNA-21 suppress ovarian tumor-associated angiogenesis in matrigel and chicken chorioallantoic membrane models

Sanaz Javanmardi[1] , Samira Sadat Abolmaali[2*] , Mohammad Javad Mehrabanpour[3], Mahmoud Reza Aghamaali[1], Ali Mohammad Tamaddon[4]

[1]Department of Biology, Faculty of Science, University of Guilan, Rasht, Iran

[2]Pharmaceutical Nanotechnology Department and Center for Nanotechnology in Drug Delivery, Shiraz University of Medical Sciences, Shiraz 71345, Iran

[3]Razi Serum and Vaccine Research Institute, Shiraz, Iran

[4]Center for Nanotechnology in Drug Delivery, Shiraz University of Medical Sciences, Shiraz 71345, Iran

Abstract

Introduction: Recently, MicroRNAs have gained increasing popularity as a novel nucleic acid-mediated medicine to regulate cancer-related protein expression. MicroRNA-21 (miR-21) is known as an oncogenic microRNA which is overexpressed in almost all cancers, including ovarian carcinoma that causes cisplatin (cis-Pt) resistance and vascular endothelial growth factor (VEGF) upregulation. So, miRNA-based therapy can be regarded as knocking down miR-21 expression, inducing tumor cell apoptosis, and suppressing tumor-associated angiogenesis.

Methods: PEG5k-carboxymethylated polyethyleneimine nanohydrogels (PEG5k-CMPEI) were loaded with AntagomiR-21 (As-21) at different ratios of nitrogen to phosphorus (N/P). Particle size and ζ potential were determined for the As-21 loaded nanohydrogels. In the cellular experiments, miR-21 expression, cytotoxicity, and cis-Pt sensitivity were studied on A2780 ovarian cancer cell lines. Finally, tumor cell apoptosis and tumor cell-associated angiogenesis were explored *in vitro* and *in vivo*.

Results: The nanohydrogels, featuring homogeneous size distribution and redox-responsiveness, were steadily loaded by As-21 at the optimum N/P ratio of 5 without any aggregation as determined by transmission electron microscopy (TEM). As-21-loaded nanohydrogels caused sequence-specific suppression of miR-21 expression and provoked apoptosis through ROS generation and caspase 3 activation. Cisplatin cytotoxicity was remarkably enhanced in A2780R as compared to A2780S following co-incubation with As-21-loaded nanohydrogels. Interestingly, the condition of the medium derived from As-21 nanohydrogel-treated A2780R cells inhibited VEGF suppression in human umbilical vein endothelial cells (HUVECs) and the formation of tubes in Matrigel. Moreover, the condition medium caused angiogenesis inhibition in the chicken chorioallantoic membrane (CAM) model.

Conclusion: These results suggest that nanohydrogel-based delivery of As-21 can be a promising neoadjuvant therapy for treating resistant tumors via apoptosis induction and angiogenesis suppression.
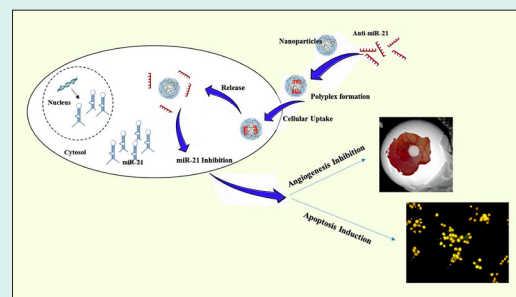
Introduction

Ovarian cancer is ranked as the 5th cause of cancer mortality and the 10th most common cancer among women in the US. Based on the reports, the 5-year survival rate of advanced ovarian cancer patients is only 30%,[1] so the development of alternative therapeutic options seems crucial. Despite the response of ovarian cancer patients to platinum chemotherapy, about one-third of these patients show resistance to cisplatin (cis-Pt).[2] Diverse mechanisms have been suggested for cis-Pt resistance, which can be divided into pump and non-pump mechanisms. In the first mechanism, the P-glycoprotein and multi-drug resistant proteins are involved. In the second mechanism, anti-apoptotic mediators like bcl-2 and survivin are

mostly responsible for turning on.[3,4] Moreover, cis-Pt resistance may coincide with increased cellular content of metallothioneins and glutathione.[5]

MicroRNAs (miRNAs) are expressed as long primary transcripts which are then transformed into mature miRNAs by several enzymatic steps. MiRNAs play fundamental roles in biological procedures involved in gene expression. Any intracellular alteration of miRNA can result in severe diseases, including different types of cancers. MicroRNA-21 (miR-21) is regarded as an oncogenic miRNA,[6] whose overexpression can down-regulate prominent tumor inhibitor proteins like programmed cell death protein 4, tumor necrosis factor α (TNFα), extracellular signal-regulated kinase (ERK), and vascular endothelial growth factor (VEGF).[7] Moreover, miR-21 overexpression can influence the content of reactive oxygen species (ROS) by targeting superoxide dismutase 3 and TNFα.[8,9] Importantly, miR-21 is significantly overexpressed in human ovarian cell lines through inhibiting PTEN expression.[10] Moreover, miR-21 upregulation is involved in cis-Pt resistance in ovarian cancer cells [7] through increasing PDCD4 expression[11] through the JNK-1/c-Jun/miR-21 pathway.[12] Therefore, it has been hypothesized that AntagomiR-21 (As-21) delivery to ovarian cancer cells could inhibit cell proliferation and tumor-associated angiogenesis through regulating ROS-mediated apoptosis.

Effective miRNA-based therapy requires a convenient delivery system to overcome the intra- and extra-cellular barriers. Several studies have addressed the application of polymeric systems for nucleic acid delivery with potential therapeutic effects on ovarian cancer cells. Zou et al introduced PLGA nanoparticles for successful knockdown of focal adhesion kinase and CD44 in nude mice with ovarian carcinoma.[13] In another study, systemic administration of amine-modified poly(α) glutamate nanoparticles was proposed as a promising carrier for silencing an essential cell-cycle protein, Plk1, in human SKOV-3 ovarian cancer.[14] Polyethyleneimine (PEI) is generally recognized as the gold standard of polymeric vector which can be modified to reduce the inherent cytotoxicity, immunogenicity, and nonspecific interactions with serum proteins. Cholesterol-modified PEG–PEI lipo-polymer is currently in clinical trials for immunotherapy of ovarian cancer through interleukin-12 overexpression.[15]

PEG-modified PEI nanohydrogels have emerged as an innovative and promising therapeutic intervention for oligonucleotide delivery. Owing to their unique core-shell structure, they can exhibit enhanced aqueous dispersion, nuclease protection, and phagocytic elimination with reduced plasma protein interactions.[16] In our previous study, it was shown that carboxymethylation of the PEG2k-PEI nanohydrogels can improve oligonucleotide delivery.[17] Redox-sensitive disulfide crosslinks of the nanohydrogels and the subsequent carboxymethylation reaction of PEI

can facilitate the intracellular release of encapsulated nucleic acids.[18] To enhance the steric hindrance property of the PEG shell which imparts biocompatibility and reduced protein instability.[19]

Our previous paper was aimed at preparing PEG2k-CMPEI nanogels for As-21 loading and sensitizing resistant tumor cells to cisplatin as evaluated by fluorescence microscopy, RT-PCR, MTT, and live/dead assays.[17] Nanogel synthesis using high instead of low molecular weight PEG, can promote the nanogel cytocompatibility and its stability against serum proteins and extracellular matrix for *in vivo* experiments. In this regard, we chose PEG5k-CMPEI for the nanogel synthesis and As-21 loading. Importantly, apart from evaluating miR-21 expression and tumor cell toxicity, the present work aimed at inducing tumor cell apoptosis (Cas3 activity), VEGF secretion, and intracellular ROS generation. Since miR-21 overexpression can be responsible for drug resistance in ovarian cancer cells,[7] the experiments were conducted on cis-Pt resistant (A2780R) ovarian cancer cells and compared with the sensitive cells (A2780S). Importantly, suppression of tumor-induced angiogenesis was assayed in Matrigel (*in vitro*) and chicken chorioallantoic membrane (CAM) *in vivo*.

Materials and Methods
Materials
Branched PEI 10 kDa and mPEG 5 kDa were respectively supplied from Poly Sciences Inc. (Canada) and Jenkem (USA). Dithiodipropionic acid (DTDP), N-hydroxysuccinimide (NHS), sodium borohydride (NaBH$_4$),1-(3-dimethylamino-propyl)-3-ethylcarbodiimide hydrochloride (EDC), 3-(4,5-dimethyl-thiazol-2-yl)-2,5-diphenyltetrazolium bromide (MTT), ethidium bromide (EthBr), cisplatin (cis-Pt), and N-acetyl-(Asp-Glu-Val-Asp)-7-amino-4-trifluoromethylcoumarin (Ac-DEVD-AFC) were provided from Sigma-Aldrich (USA).

A2780S and A2780R cell lines and human umbilical vein endothelial cells (HUVECs) were provided from Pasture Institute (Iran, Tehran). As-21 and scrambled sequences were TCAACATCAGTCTGATAAGCTA and CATTAATGTCGGACAACTCAAT, respectively.

Synthesis of nanohydrogels
Synthesis of the nanohydrogels (NG) was carried out through two steps: 1) preparation and redox-sensitive crosslinking of PEG5k-PEI, and 2) carboxymethylation reaction (Fig. 1). Briefly, the NHS-activated ester solution of mPEG$_{5000}$–COOH in methanol was prepared and added to PEI solution in dichloromethane at the weight ratio of 0.5 under 3-hour stirring. Then, a rotational speed vacuum was used to concentrate the products which were subsequently diluted in distilled water, dialyzed using a Float-A-Lyzer (6–8 kDa), and lyophilized. The crosslinking was achieved by dissolving 30 mg PEG5k-PEI in 100 mM
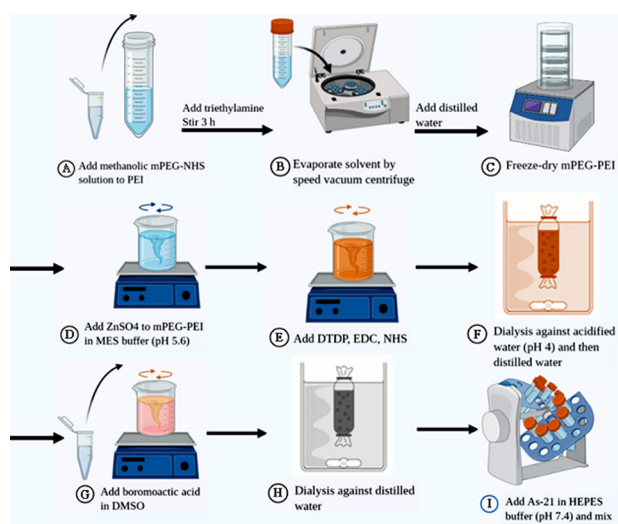
Fig. 1. Illustrated scheme for the synthesis of PEG5k-CMPEI NG and As-21 loading. (A) NHS-activated ester of mPEG5000–COOH solution in methanol was added to PEI solution in dichloromethane; (B) the products was concentrated using rotational speed vacuum and diluted in distilled water and (D) lyophilized; (E) the crosslinking reaction was achieved by dissolving PEG5k-PEI in MES buffer (pH 5.6) containing ZnSO4 ; (F) then, DTDP, EDC, and NHS in DMSO was added to the reaction vessel; (G) the mixture was dialyzed against HCl solution (pH 4.0) and then in distilled water; (H) bromoacetic acid was added for modifying NG to PEG5k-CMPEI NG; (I) the products were stirred overnight followed by dialysis for 3 days against distilled water; and (9) As-21 loading thourgh incubating PEG5k[1]CMPEI NG with As-21 solution in HEPES buffer (pH 7.4); mPEG, methoxy polyethylene glycol; NHS, N-hydroxysuccinimide; PEI, poly ethyleneimine; MES, 2-(N-morpholino)ethanesulfonic acid; DTDP, dithiopropionic acid; EDC, 1-(3-dimethylamino-propyl)-3-ethylcarbodiimide hydrochloride; HEPES, 4-(2-hydroxyethyl)-1-piperazineethanesulfonic acid.

MES buffer (pH=5.6) followed by dropwise addition of ZnSO$_4$ solution. The reaction continued by adding 100 mM DTDP solution in DMSO, EDC, and NHS (the respective molar ratio: 2:2:1). After 24-hour stirring, the mixture was dialyzed against HCl solution (pH 3.0), and then distilled water. For the synthesis of the carboxymethylated NG (PEG5k-CMPEI NG), bromoacetic acid (12 mg in 3 ml DMSO) was added to NG (4 ml, 2.5 mg/mL). The products were stirred overnight followed by dialysis for 3 days against distilled water.

Characterization of nanohydrogels

Infrared spectroscopy was carried out (Vertex, Bruker, Germany) to assess the variations in the structure of PEG5k-PEI following the crosslinking reaction and carboxymethylation. Sample preparation involved geometric dilution of equal amounts of the lyophilized products and potassium bromide followed by their compression into discs. Twenty scans were averaged at the resolution of 4 cm^{-1} in the range of 500- 4000 cm^{-1}. ^{1}H-NMR spectroscopy of nanohydrogels (Bruker-400 MHz) was achieved by D$_2$O solvent. The degree of carboxylation was determined based on the proton integration method. Since the carboxymethylation reaction often involves

the PEI primary amines,[20] changes in primary amine concentration of nanohydrogels were determined by TNBS assay [21] at the equivalent polymer concentration of 0.75 mM PEI. Briefly, 2.6 μL of TNBS reagent was added to a 0.5 mL sample diluted in 0.1 M borate buffer (pH 9.5). After 45-minute incubation at 25°C, the absorbance was read at the wavelength of 420 nm by UV–visible spectroscopy (ELISA reader, BioTek, USA). The concentration of primary amines was calculated from the calibration curve plotted for glycine standard solutions. For calculating the carboxymethylation degree, the amine concentration of PEG5k-PEI NG was divided by the one calculated for PEG5k-CMPEI NG at similar PEI molar concentrations (0.75 mM). Ellman's assay was carried out to determine the degree of redox-sensitive crosslinking, performed.[22] In a typical procedure, 25 μL NaBH$_4$ (0.2 M) in 0.2% NaOH (as the reducing agent) was added to 45 μL samples (at a nominal concentration of 4 mM total amines) which were incubated for 1 h. The mixture volume was increased to 90 μL using 300 mM HEPES buffer (pH=8). Subsequently, 10 μL DTNB solution (4 mg/mL, Ellman's reagent) was added. Following 15-minute incubation, the absorbance was measured at 412 nm. The calibration curve was plotted for the reduced glutathione standard solutions and the free thiol concentration was calculated from the calibration curve.

Preparation and evaluation of As-21-Loaded NG (Nanoplexes)

Nanoplexes were synthesized through direct mixing of oligonucleotide sequences (As-21 or Scr) with PEG5k-CMPEI NG at different N/P ratios. The product was further incubated for 0.5, 3, 6, and 24 hours at 25°C. Agarose gel retardation assay was conducted using a Bio-Rad electrophoresis apparatus at 60 V, for 30 minutes in 2.5% (w/v) agarose gel, and visualized on a UV trans-illuminator. For investigating the biological stability against nucleases, As-21/NG Nanoplexes (containing 3 μg DNA at the N/P=5) were incubated with 2 μL 10X reaction buffer and 2 U of DNase I. The mixture was then incubated at 37°C for 1, 3, 6, and 24 hours. An aliquot was run at 2.5% agarose gel electrophoresis and its stability against DNase I was compared with the naked As-21. EthBr dye exclusion assay was carried out to assess the stability of As-21/NG nanoplexes against polyanionic heparin sulfate simulating the extracellular matrix. Briefly, to each well of a 96-well plate containing nanoplexes with various N/P ratios, 1 IU heparin sulfate was added per μg of the oligonucleotide. Following 15-minute incubation in dark, 50 μL EthBr (1 μg/mL) was added and fluorescence intensity was measured at the respective excitation and emission wavelengths of λ = 510 and 595 nm. Oligonucleotide efflux (%) was calculated from fluorescence intensities prior to and after adding heparin sulfate.

Size, zeta-potential, morphology, and serum stability

Hydrodynamic diameters of the PEG5k-CMPEI NG (intact or reduced) and As-21/NG Nanoplexes (at N/P= 5) were determined in 10 mM phosphate buffer (pH 7.4) by dynamic light scattering method (Nanoflex DLS 180˚, Particle Metrix, Germany). ζ-Potential measurements were also conducted using ZETA-Check (Microtrac, Germany). Morphology of As-21/NG nanoplexes was investigated using transmission electron microscopy (TEM, Zeiss-EM10C-80KV, Germany) after negative staining by 1% uranyl acetate solution.

To investigate the serum stability of PEG5k-CMPEI NG *vs.* PEI or PEG5k-PEI copolymer, 100 μL of each polymer dispersion (1 mg/mL) was added to 96 well-plate. UV-Vis spectrophotometry was employed to measure the background absorbance (A_0) at λ = 420 nm. A rising volume of human serum albumin (HSA) (20 mg/mL) was added to each well to obtain different concentrations ranging from 1-20%, then the absorbance (A) was read after a 10-minute incubation at 25°C.[23]

Cell culture and transfection

The cells were cultured in an RPMI medium supplemented with 10% FBS and 1% antibiotic at 37°C in a humidified atmosphere with 5% CO_2. The aliquots of 0.1 μM cis-Pt were added to the A2780R culture medium after each passage to maintain the phenotype resistance. For suppression of miR-21, naked As-21 (as a single-stranded deoxyribonucleic acid chain) and As-21-loaded nanohydrogels (As-21/NG) were used to transfect A2780S and A2780R. Other samples included naked scrambled sequence (Scr), scrambled loaded NG (Scr/NG), NG, and untreated control.

MTT assay

2.5×10^4 A2780R and A2780S cells were seeded in 96-well plates and incubated at 37°C and 5% CO_2 for 24 hours. They were then exposed to different levels of PEG5k-CMPEI NG. The MTT assay was conducted to explore the sequence-specific growth inhibition after 72-hour treatment with As-21/NG *vs.* Scr/NG (N/P = 5). After 3-hour incubation with 100 μL MTT (0.5 mg/mL) in PBS at 37°C, the optical absorbance of the cells was determined (at 570 nm referencing 690 nm) following the addition of 0.1 mL DMSO. Cell viability was determined as the percentage relative to the controls.

miR-21 expression assay by stem-loop RT-PCR

Following 24-hour incubation, the seeded cells were treated with As-21, Scr, As-21/NG (N/P = 5), Scr/NG (N/P = 5), or unloaded NG for 72 hours. The total RNA was extracted based on the Dena Zist Asia Kit instruction. cDNA was synthesized by M-MuLV-Reverse Transcriptase and a special stem-loop primer for microRNA-21 (CACCGTTCCCCGCCGTCGGTGTCAACA) (30 minutes 16°C, 60 minutes 42°C followed by 10 minutes

at 70°C). The PCR involved: 94°C for 2 minutes, followed by 40-60 cycles of 93°C for 30 seconds, 58°C for 1 minute, and 72°C for 30 seconds. Forward and reverse primer sequences were CCCGCCTAGCTTATCAGACTG and GCCGTCGGTGTCAACATCA, respectively. As an internal control, β-actin expression was determined as reported in the literature.[24,25] The product was run on 2% agarose gel at 60 V for 30 minutes and analyzed using ImageJ software.

Influence of miR-21 downregulation on cis-Pt resistance

The impact of As-21/NG treatment on cis-Pt resistance was evaluated by the treatment of A2780S and A2780R with As-21/NG. After 48 hours, the medium was aspirated and replaced by the medium containing 5 or 10 μM cis-Pt. Cell viability was determined after 24 hours post-incubation by the MTT assay.

Reactive oxygen species (ROS)

Intracellular levels of ROS were assessed using dichloro-dihydro-fluorescein diacetate (DCFH-DA). DCFH-DA can enter the cells, and react with ROS, giving rise to a fluorescent compound, dichlorofluorescein (DCF). A2780S and A2780R (1.5×10^4 cell/well) were treated with As-21/NG or Scr/NG for 72 h followed by one-hour incubation with 1 mL of 100 μM DCFH-DA solution at 37°C. Then, the fluorescence was determined at the respective excitation and emission wavelengths of 485 and 530 nm.

Acridine orange (AO)/ EthBr double staining

AO/EthBr double-staining assay was performed for differentiation of alive, apoptotic, and necrotic cells. The seeded A2780S and A2780R cells (5×10^5 cells/well in 24-well plates) were treated with As-21/NG or Scr/NG at N/P = 5. After 72 hours, they were trypsinized, stained by a mixture of AO/EthBr (with the concentrations of 100 μg/mL AO and EthBr each in PBS), and evaluated by fluorescent microscopy (Nikon Eclipse E400, Japan). The number of apoptotic cells was counted in 400x magnification and compared with the total number of cells. The average percentage of apoptotic cells was calculated from 3 different microscopic fields of view and compared for various treatments.

Caspase 3 (Cas3) activity assay

To investigate apoptotic cell death caused by As-21/NG or Scr/NG in A2780S and A2780R cells, Cas3 activity was evaluated using 7-amino-4-trifluoromethyl coumarin (AFC) colorimetric assay. Briefly, 4×10^6 treated cells were lysed on ice and cell protein content was determined by Bradford reagents. Cell lysate proteins (200 μg) were then added to the Ac-DEVD-AFC reagent and incubated at 37°C for 1 hour. Cas3 expression and its relative concentration were calculated using the calibration curve obtained for various concentrations of Ac-DEVD-AFC

at 450 nm. Fold enhancement in Cas3 activities was calculated by comparing the fluorescence intensity of each sample with the untreated control group.

Angiogenesis assay

To evaluate the antiangiogenic effect of As-21/NG, A2780 cells were treated with As-21, As-21/NG, Scr, Scr/NG (N/P = 5), or NG (at concentrations equal to 100 µM As-21 or Scr) for 72 hours. The conditioned cell culture medium was collected by centrifugation at 1000 rpm and the secreted angiogenic factors were concentrated 20X using an Amicon ultrafiltration device (30 kD).[26] Afterward, VEGF secretion, *in-vitro* endothelial cell tube formation, and *in vivo* neovascularization in the CAM were investigated, as will be explained in the following sections.

Enzyme-linked immunosorbent assay (ELISA) for VEGF secretion

VEGF secretion by the HUVEC cells was evaluated by the VEGF ELISA Assay Kit (Invitrogen, USA) as mentioned by the manufacturer's instruction. Typically, 10^4 cells were seeded in DMEM-F12 medium containing 1% FBS at 37°C for 72 hours. VEGF concentration in the cell culture was determined using the calibration curve obtained from standard VEGF solutions at 450 nm, using UV–visible spectrophotometer.

Endothelial cell tube formation assay

For tube formation assay, each well of the 96-well plates was coated with 50 µL Matrigel (BD Biosciences, USA) and left to polymerize for 45 minutes at 37°C. Then, 8×10^4 HUVEC cells were seeded on the Matrigel-coated wells in DMEM-F12 medium containing 1% FBS at 37°C. Cells start forming tubes even after 2-hour incubation with the conditioned medium of A2780R or A2780S cells. The images were taken after 6 hours by a digital camera attached to an inverted phase-contrast microscope.[27]

CAM assay

Animal tests were conducted according to Codes of Ethics and Practice approved by the Institutional Animal Care and Use Committee in line with the guidelines of Shiraz University of Medical Sciences (SUMS). Fertilized chicken eggs were kindly donated by Razi Serum and Vaccine Research Institute and incubated at 37°C with 70% humidity for 9 days. A window was created above the air sac and 0.25 cm-diameter filter papers were used on the surfaces of the CAM and which were soaked with 30 µL of conditioned medium of A2780 cells. After sealing the windows, the eggs were incubated for 3 days. The CAMs were cut and fixed with formalin and the length and width of the blood vessels were analyzed using ImageJ software.[28]

Statistical analysis

Statistical analysis of the data was achieved by Prism software version 5.0 (GraphPad, USA). *P* values < 0.05 were considered statistically significant. The data were reported as mean ± SD.

Results

Physicochemical characterization of the nanohydrogels

PEG5k-CMPEI NG was synthesized and evaluated by FTIR and ^{1}H-NMR spectroscopy (Supplementary file 1). A distinct broad peak at 2500- 3000 cm^{-1} in the FTIR spectrum can be assigned to the hydroxyl group of carboxylic acid [29] and the peaks emerging at 3420, 1113, and 1669 cm^{-1} could be also linked to N-H, C–O, and amide C=O stretching of PEI, PEG5k and DTDP, respectively.[18] ^{1}H-NMR was utilized to calculate the degree of PEI carboxylation. The peaks at 3.4 and 2.3- 3.3 ppm can be attributed to CH_2-O of PEG and CH_2-N of PEI, respectively. Moreover, the peak of CH_2-CH_2-COOH appeared at 2.3-3.3 ppm. TNBS assay showed the concentration of PEG5k-PEI primary amines reduced from 8.9 to 4.1 mM after the crosslinking reaction to produce NG. In addition, the primary amine concentration of PEG5k-CMPEI NG was determined about 0.7 mM, indicating a successful carboxymethylation reaction (about 83% reduction in the primary amine concentration). The concentration of PEI amines consumed in the carboxymethylation reaction decreased from 6.57 to 2.02 mM (unpublished ninhydrin assay data), indicating a carboxymethylation degree of about 69%. In parallel, Ellman's assay showed that, unlike the intact NG which contained disulfide crosslinks, free thiol concentration of $NaBH_4$-reduced PEG5k-PEI NG and PEG5k-CMPEI NG were 0.15 and 0.11 mM, respectively. The recovered free thiols were similarly consistent with the calculated crosslink density of 7.5%.

Particle size, morphology, and stability

Particle size and ζ potential were evaluated before and after reducing the crosslinker with $NaBH_4$ and after As-21 loading at N/P = 5. The particle size of PEG5k-PEI and PEG5k-CMPEI NG was determined 382 ± 0.43 and 267 ± 0.23 nm with the corresponding ζ potential values of +23.0 ± 1.3 and +17.7 ± 1.7 mV, respectively (Table 1). Interestingly, following $NaBH_4$ treatment, the particles disappeared (Fig. 2A), confirming the redox sensitivity of NG. After As-21 loading (N/P = 5), As-21/NG nanoplexes exhibited a uniform size of 197 ± 0.32 nm and a shift was observed in the ζ potential from +17.7 ± 1.7 (NG) to -4.2 ± 1.3 mV (As-21/NG). TEM experiment showed

Table 1. Intensity size, polydispersity index (PDI) and ζ potential (mean ± SD) of polycations alone and after As-21 loading at N/P=5

	Intensity size (nm), PDI	ζ Potential (mV)
PEG5k-PEI	382, 0.43	+23.2 ± 1.3
PEG5k-PEI/As-21	297, 0.23	-40.1 ± 4.2
PEG5k-CMPEI	267, 0.23	+17.7 ± 0.7
PEG5k-CMPEI/As-21	197, 0.32	-4.27 ± 1.3
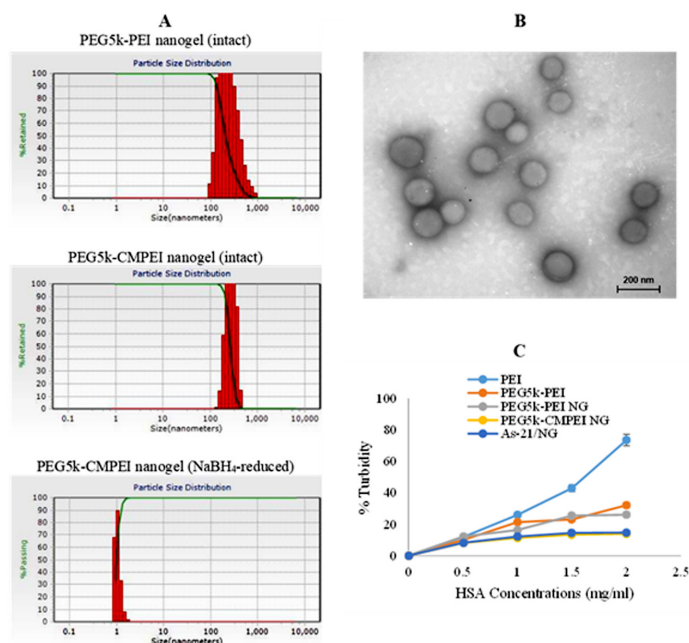
Fig. 2. Nanohydrogels characterization: (A) intensity-size distribution of PEG5k-PEI and PEG5k-CMPEI NG, either intact or reduced with NaBH$_4$, (B) negative-stain TEM image of As-21/ PEG5k-CMPEI NG at N/P=5, and (C) turbiditiy of NG *vs.* PEI or PEG5k-PEI at different HSA concentrations.

discrete, small, and spherical As-21/NG nanoplexes (Fig. 2B). The turbidimetric assay was performed to examine the stability of PEG5k-CMPEI NG *vs.* PEI and PEG5k-PEI copolymer or PEG5k-PEI NG in the presence of HSA. Fig. 2C shows increased turbidity of PEI, PEG5k-PEI, or PEG5k-PEI NG at concentrations above 0.5 mg/mL HSA. Unlike PEG5k-PEI NG which showed significant turbidity at HSA concentration of 1 mg/mL ($P <0.0001$), no significant turbidity was detected in PEG5k-CMPEI NG over a wide range of concentrations, either before or after As-21 loading, confirming the nanohydrogel stability against HSA.

Agarose gel retardation assay

As-21 loading was determined by agarose gel electrophoresis. As shown in Fig. 3A, the As-21 band was retained in the gel after increasing both the N/P ratio and the incubation time until no free oligonucleotide band was observed in the gel, which can be referred as the optimum condition for oligonucleotide loading.[30] To evaluate the stability of As-21/NG against nuclease and polyanion-induced displacement, DNase I digestion and heparin sulfate competition assays were performed. Fig. 3B showed almost complete protection of As-21 by NG (N/P = 5) against enzymatic degradation even after prolonged incubation times. Furthermore, as shown in Fig. 3C, no significant oligonucleotide efflux was recognized for As-21/NG prepared at N/P ratios > 2, indicating complete protection of As-21 against the extracellular matrix.[31] Although almost complete retention of As-21 in the gel was found after loading in NG at the N/P ratio = 0.5, As-21 protection against DNase I digestion and retention in presence of heparin sulfate were successfully attained

at N/P ratio = 5. Hence, the N/P = 5 was chosen as the optimum formulation.

MTT assay

MTT assay was carried out first for investigating the sequence-specific cytotoxicity of As-21/NG Nanoplexes. As a control experiment, no significant toxicity was found in the unloaded NG at concentrations lower than 50 µg/mL ($P < 0.01$) (Fig. 4A). Nonetheless, the cytotoxicity was enhanced by increasing the polymer concentration so that significant cytotoxicity was detected at concentrations as low as 100 µg/mL in A2780S ($P < 0.005$) and A2780R ($P < 0.001$). Subsequently, inhibition of cell growth induced by As-21/NG was explored by changing the N/P ratios (N/P = 1, 2, and 5) in A2780S and A2780R cell lines. According to Fig. 4B, unlike As-21 or NG, As-21/NG exhibited a significant reduction in cell viability. Indeed, As-21/NG did not exhibit significant cytotoxicity at N/P=1 and 2; the viability however decreased significantly in both cell lines at N/P=5. Compared to NG, treating the cells with As-21/NG at N/P = 5 resulted in a decreased cell viability by 51% ($P < 0.0001$) and 59% ($P < 0.005$) in A2780S and A2780R, respectively. Importantly, the Scr/NG did not cause any significant cytotoxicity.

Our preliminary study revealed no significant cytotoxicity of cis-Pt on A2780S or A2780R at concentrations lower than 20 µM (data not shown). However, as shown in Fig. 4C, the cells pre-treated for 48h with the As-21/NG exhibited remarkable cytotoxicity even in sub-toxic cis-Pt concentrations (5 and 10 µM). The cytotoxicity was more pronounced in A2780R compared to A2780S ($P < 0.0001$).
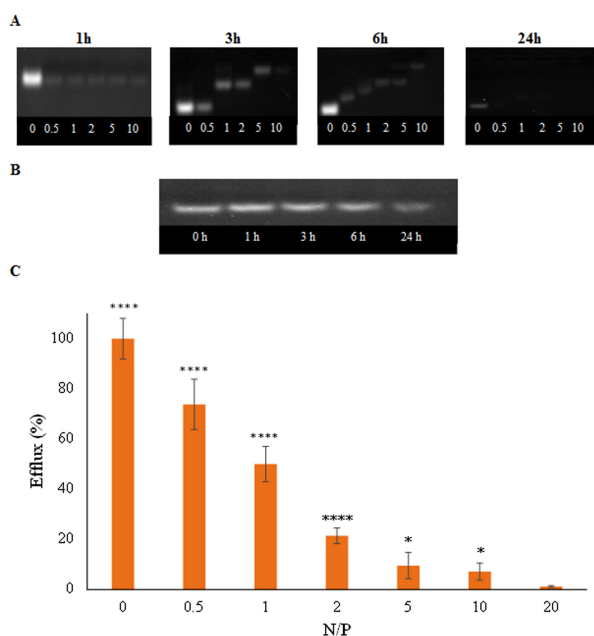
Fig. 3. Formation of As-21/NG nanoplexes: A) gel retardation assay at various incubation times and N/P ratios (from left to right: 0, 0.5, 1, 2, 5, 10), B) DNase I digestion assay in agarose gel at various incubation times (from left to right: 0, 1, 3, 6, 24 h), C) polyanion competition assay after adding 1 U heparin sulfate to As-21/NG nanoplexes at various N/P ratios (3 replicates); * $P < 0.05$; **** $P < 0.0001$.

Fig. 4. MTT-based cytotoxicity of A) PEG5k-CMPEI NG, B) various N/P ratios of As-21/NG and Scr/NG, C) As-21/NG (N/P=5) plus cis-Pt on A2780S and A2780R cells. Asterisks indicate significant cytotoxicities; * $P < 0.05$; ** $P < 0.01$; *** $P < 0.001$; **** $P < 0.0001$.

miR-21 expression

As shown in Fig. 5A, the relative expression of miR-21 was reduced after treating A2780S or A2780R cells with the As-21/NG, whereas the Scr/NG or As-21 did not show any significant effects. Gene silencing efficiency was higher in A2780R. Moreover, no substantial change was determined in the expression of ß-actin (as the housekeeping gene) (Fig. 5B).

Double-stained fluorescence microscopy

Morphological alterations (cell shrinkage, chromatin condensation, and nuclear fragmentation) in the treated cells were detected by AO/EthBr double fluorescent staining. As shown in Fig. 6A, high percentages of live cells (96% ± 7.9) with normal morphology can be detected in the Scr and As-21 groups. Interestingly, early and late apoptotic cells could be detected in the As-21/NG-treated cells (32% ± 2.4 and 56% ± 4.6 of live cells in A2780R and A2780S, respectively). Early apoptotic cells were recognized in the NG-treated cells (86% ± 6.2). Thus, As-21/NG could remarkably enhance the cell membrane permeability toward EthBr in both A2780S and A2780R cell lines.

ROS and Cas3 activity assays

Cas3 enzymatic activity was determined to assess the apoptotic effect of As-21/NG. Compared to the control groups, As-21/NG increase caused a 2.81 (P <0.001) and 2.04 (P <0.01) fold enhancement in the Cas3 activity in

A2780R and A2780S, respectively (Fig. 6B). Also, Cas3 activation was more noticed in A2780R (P<0.05). DCF fluorescence was determined to investigate the possible role of ROS generation in induced apoptosis. AS-21/NG caused a significant increase in the ROS concentration (approximately 2.82 and 2.30 folds in A2780R and A2780S cells, respectively) (Fig. 6C). Similar to the untreated control group, no significant ROS production was found in As-21, Scr, Scr/NG, or unloaded NG groups, indicating sequence-specific ROS-mediated induction of apoptosis in As-21/NG-treated A2780S and A2780R cells.

VEGF, matrigel and CAM assays

Fig. 7A shows a remarkable suppression in VEGF production after As-21/NG treatment as compared to the untreated control group. Moreover, this inhibition was more pronounced in A2780R (P < 0.001) than A2780S (P < 0.05). Interestingly, the Scr/NG caused no significant changes in VEGF expression, indicating the sequence-specific inhibition of VEGF expression. Regarding endothelial cells tube formation, Fig. 7B and Fig. 7C suggest that the conditioned cell culture medium isolated from the untreated control as well as Scr and NG groups can induce tube formation; however, a significant decline

A

B

C
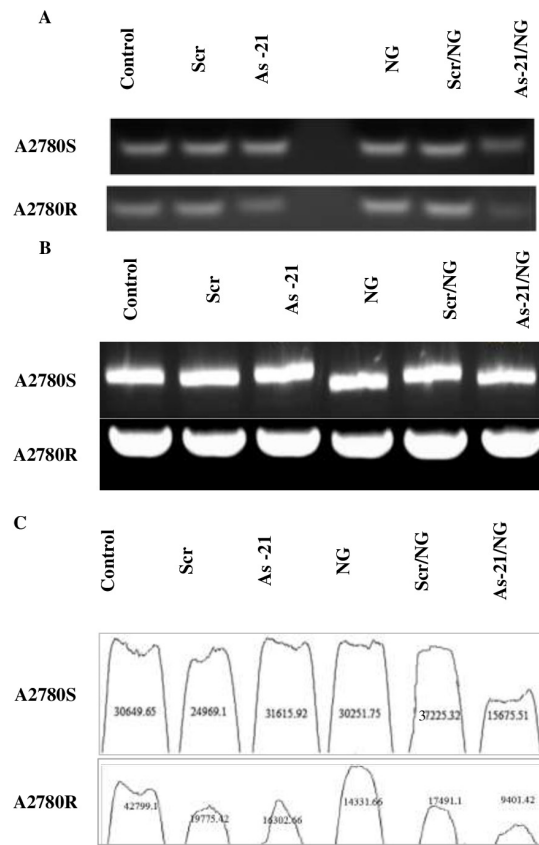
Fig. 5. A) miR-21 and B) β-actin expression in A2780S and A2780R cells treated with As-21/NG, Scr/NG, As-21, or Scr *vs.* untreated control. C) ImageJ analysis of miR-21 expression in A2780S and A2780R cells treated with As-21/NG, Scr/NG, As-21, or Scr *vs.* untreated control.
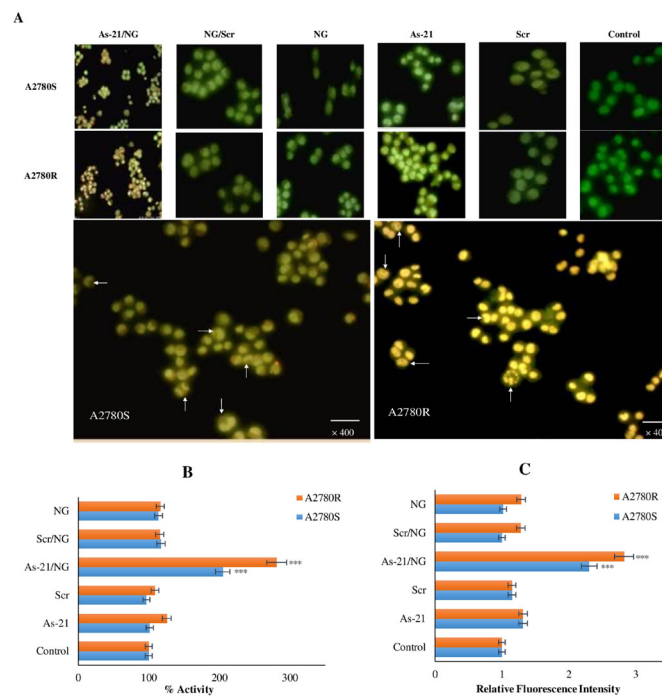
Fig. 6. A) AO/EthBr double-stained images of A2780S and A2780R cells treated with As-21/NG, Scr/NG, As-21 or Scr *vs.* untreated control; green live cells, yellowish-green early apoptotic cells with nuclear margination and chromatin condensation, and orange late apoptotic cells with fragmented chromatin and apoptotic bodies. Arrows show the fragmented chromatin and apoptotic bodies in the As-21/NG treated cells, B) Cas3 activity, C) ROS generation. Asterisks indicate significant differences with untreated controls; *** $P < 0.001$; **** $P < 0.0001$.
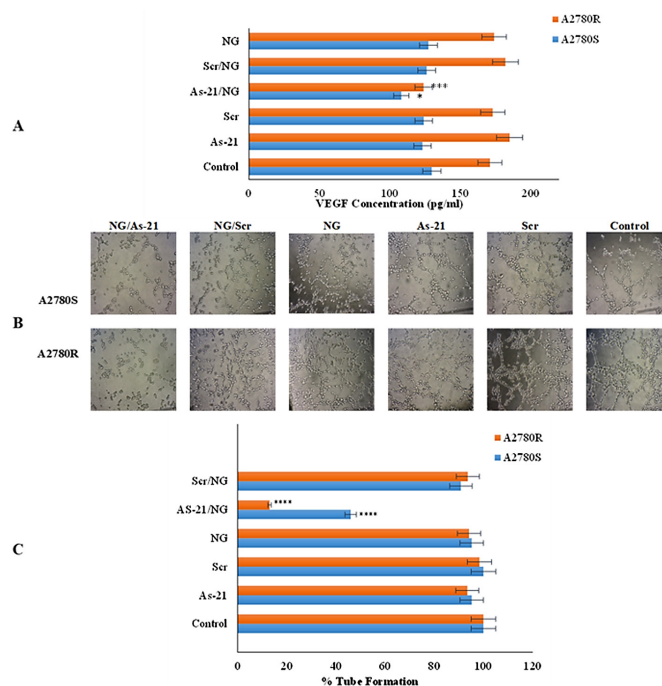
Fig. 7. Effect of As-21/NG on A) VEGF secretion by A2780S and A2780R cells and B) HUVEC tube formation in Matrigel® (100x magnification). Asterisks indicate significant differences with untreated controls; * $P < 0.05$; *** $P < 0.001$; **** $P < 0.0001$.

was observed in tube formation of the As-21/NG-treated cells (54% and 87% inhibition in A2780S and A2780R, respectively). Moreover, tube formation was not affected by Scr/NG or NG treatment.

The CAM assay was also carried out to investigate the effect of As-21/NG on *in vivo* angiogenesis. Compared with Scr/NG, incubation with the As-21/NG inhibited new blood vessels and reduced the width of the blood vessel (Fig. 8A and Fig. 8B). Furthermore, after treatment with As-21/NG, the conditioned media of A2780R and A2780S cells caused angiogenesis inhibition (79% ± 5.8 and 23% ± 4.2, respectively). Similarly, the width of the blood vessel was effectively decreased in A2780S and A2780R by 43% ± 6.8 and 83.9% ± 9.1, respectively. Thus, angiogenesis suppression was more pronounced in the resistant phenotypes.

Discussion

In this research, the design and applicability of As-21/NG for tumor-induced angiogenesis suppression were addressed. Regarding the possible role of miR-21 overexpression in the chemotherapy resistance of the ovarian cancer cells,[7] the biologic effects of As-21/NG were investigated in both sensitive (A2780S) and cis-Pt-resistant (A2780R) ovarian carcinoma cell lines.

The successful synthesis of PEG5k-CMPEI NG was confirmed by FTIR and ¹H-NMR. NG featured modulated amine content and redox responsiveness according to biochemical assays and DLS (Fig. 2A). First, successive alterations in free amine residues were shown by TNBS assay.[32] Similarly, the crosslinking reaction through acylation of the primary amines and subsequent

carboxymethylation decreased the primary amines of PEI to less than 10%. However, secondary and tertiary amine contents were enhanced through carboxymethylation resulting in incremented buffering capacity and reduced polycations-induced cytotoxicity.[33]

Ellman's assay was employed to determine the redox sensitivity of the disulfide-containing crosslinks. In contrast to intact NG, $NaBH_4$ decreased the crosslinks leading to the free thiol concentration corresponding to a 7.5% crosslinking degree. Moreover, NG with a mean size of 267 nm disintegrated after $NaBH_4$ reduction of crosslinks with no detectable particle as shown by DLS (Fig. 2A).

Before As-21 loading, the cellular toxicity of NG was investigated. Polycations cytotoxicity is a challenge in gene transfection. NG showed no significant cytotoxicity at the concentration of 50 µg/mL in both A2780S and A2780R cell lines (Fig. 4A) which is remarkably less than the unmodified PEI or uncrosslinked PEG-PEI copolymer.[34] These results are probably due to the lower primary amine content and the core-shell structure of PEG stabilized nanohydrogels.[33] These findings are comparable to our previous report on L-histidine substitution in PEG2k-PEI polymer.[35]

The binding of serum proteins to polycations can result in protein-particle aggregation [36] which is another challenge in successful mammalian cell transfection. As shown in Fig. 2C, unlike unmodified PEI and PEG5k-PEI, no significant albumin aggregation was determined for PEG5k-CMPEI NG due to the reduced positive charge of PEI as well as stabilizing action of the PEG chains. It is suggested that the steric interference of mPEG chains can
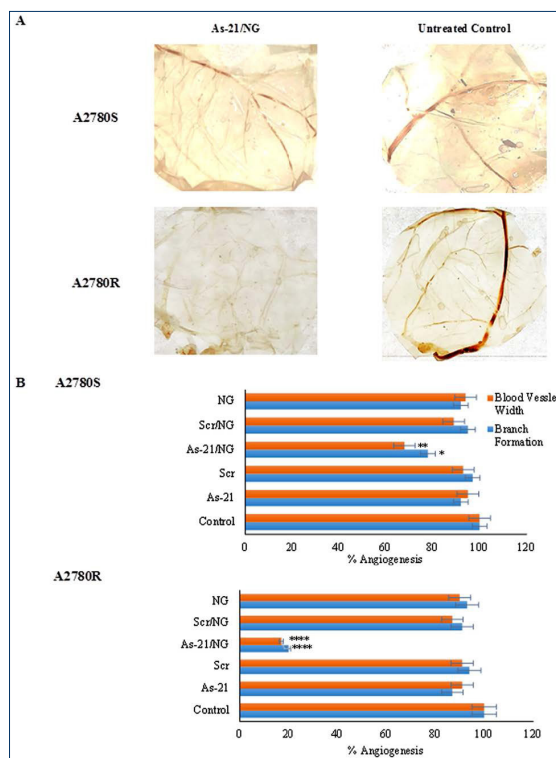
Fig. 8. Effect of As-21/NG on angiogenesis in chicken chorioallantoic membrane (CAM). Asterisks indicate significant differences with untreated controls; * P < 0.05; ** *P* < 0.01; **** *P* < 0.0001.

decline the interactions with plasma protein, giving rise to resistance against serum protein-induced aggregations.[23]

Following incubation with As-21, NG-loaded and condensed As-21 resulted in the positive charge neutralization (ζ potential= -4.2 ± 1.3 mV). Agarose gel electrophoresis was routinely used to obtain the optimum N/P ratio, which depended on the polycationic nature and chemical modifications.[37] In our experiment, the migration of the As-21 band was delayed in the gel and no migration was noticed after 24-hour incubation at the N/P ratio of 5, representing almost complete loading of As-21 in NG through electrostatic complex formation.[23]

The biological stability of Nanoplexes against DNase I and heparin sulfate displacement can be attributed to polymer structure and N/P ratio.[31] It was found that NG significantly stabilized As-21 against DNase I degradation, even after prolonged incubation times. This is possibly due to the slow diffusion of high-molecular-weight nucleases into the PEGylated nanohydrogel.[38] EthBr dye exclusion assay was also employed to assess the biologic stability of As-21/NG against heparin sulfate. EthBr intercalation with As-21 resulted in an intense fluorescence which was subsequently decreased by NG loading. NG could protect As-21, thereby excluding intercalation with the fluorescent probe. As shown in Fig. 3C, free As-21 decreased progressively by increasing the N/P ratio, suggesting the reduced accessibility of EthBr. Importantly, after adding heparin sulfate at the N/P ratio of 5, a slight efflux of the loaded As-21 was observed, confirming the stability of As-21/NG against extracellular polyanions. However, heparin

sulfate displaced As-21 at N/P ratios less than 5 which could be due to inefficient oligonucleotide condensation at low NG concentration.

Particle size, as well as ζ potential, can determine the stability, compatibility, and transfection activity of the nanohydrogels. The particle size decreased following the carboxylation reaction due to the formation of salt bridges between amines and carboxylate moieties in the NG core. Interestingly, particles with low ζ potentials in the range of -30 and +30 mV are considered stable. After incubating NG with As-21, reduced particle size and ζ potential were detected due to partial charge neutralization.[39] Although the ζ potential of As-21/NG (-4.2 ± 1.3 mV) was lower than -15 mV, no aggregation was recognized using DLS. Similarly, discrete and uniform particles were found by TEM analysis (Fig. 2B), confirming the possible stabilizing role of PEG chains.

Gel retardation assay was performed to investigate the As-21/NG formation in various N/P ratios.[40] The optimum N/P ratio depends on several factors such as the polycation nature and chemical modifications.[37] At low N/P ratios of 0.5-1, the NG was not enough for neutralizing and condensing the negatively charged As-21 even after long incubation times.[30] However, upon increasing the N/P ratio and incubation time, the migration of As-21 was more retarded in the gel so that no migration was found for the N/P = 5 after 24 hours. These results indicate neutralization of As-21 negative charge mainly through electrostatic interaction (Fig. 3A). In parallel, the stability of As-21/NG nanoplexes prepared

at N/P = 5 was investigated against DNase I. Due to the crosslinked nature of NG and the steric hindrance effect of high molecular weight PEG 5 kDa, NG showed almost complete protection of As-21 against nuclease degradation even after long incubation times (Fig. 3B). Indeed, the slow penetration of high molecular weight nucleases into the nanogel network covered by high MW PEG chains can retain As-21 integrity.[41] This result was confirmed by the stability of As-21/NG against heparin sulfate at the N/P ratio of 5 and beyond (Fig. 3C).

To determine the transfection efficiency, miR-21 expression was explored by stem-loop RT-PCR. Fig. 5A shows that miR-21 was remarkably reduced after exposure to As-21/NG as compared to As-21 and Scr groups. This effect can be attributed to the shielding of As-21 negative charge by loading in the NG, which can increase the cellular uptake as reported before.[42] Analysis using ImageJ software showed that As-21/NG treatment reduced miR-21 expression by about 59% and 78% in A2780S and A2780R cell lines, respectively (Fig. 5C). The higher sensitivity of A2780R to As-21 as also revealed for the naked sequence can be attributed to different expression levels of miR21 in sensitive and resistant cell lines. In this regard, Echevarría-Vargas et al reported that miR-21 is highly expressed in A2780R compared with A2789S which can contribute to A2780 resistance to cis-Pt[12]; therefore, it was hypothesized that knockdown of miR-21 expression can sensitize A2780R cells by inhibiting PTEN expression and JNK-1/c-Jun/miR-21 pathway.[12] Interestingly, As-21/NG (N/P = 5) showed more specific cytotoxicity in A2780R than A2780S cells (Fig. 4B). Indeed, A2780R has higher sensitivity to As-21/NG than A2780S which can be assigned to the aberrant miR-21 expression in A2780R (Fig. 5A).[12] Moreover, the results showed that the cells pre-treated with the As-21/NG can remarkably augment cis-Pt-induced cytotoxicity even at sub-toxic drug concentrations (Fig. 4C). For elucidating the mechanism(s) of As-21/NG-induced cytotoxicity, AO/EthBr staining and ROS assay experiments were performed. Results revealed morphological alterations in the cell membrane of the ovarian cancer cells treated with As-21/NG (Fig. 6A). Furthermore, As-21/NG caused an increase in the intracellular level of ROS, which resulted in Cas3 activations (Fig. 6B and Fig. 6C). It has been reported that increasing the cellular level of miR-21 mediates ROS generation through activating ERK/nuclear factor-κB (NF-κB) signal pathways.[9] Therefore, oxidative stress mediation by ROS generation can be regarded as an initiating signal of apoptosis induction by As-21[43] and subsequent Cas3 activator.

It has been reported that miR-21 induces tumor-associated angiogenesis through targeting PTEN, activation of AKT, and ERK1/2 signaling pathways, thereby enhancing HIF-1α and VEGF expression.[44] Additionally, an increased miR-21 level can activate STAT3 which increases VEGF secretion.[45] Hence, miR-21 is involved in

Research Highlights

What is the current knowledge?

√ MicroRNAs can be used for regulating expression of the cancer related proteins.

√ Overexpression of microRNA-21 (miR-21) can lead to down-regulation of the critical tumor suppressor proteins.

√ Anti-miR21 nucleic acid delivered by the nanohydrogels sensitizes resistant ovary tumor cells to cisplatin.

What is new here?

√ Carboxymethylated PEG5k-polyethylenemine nanohydrogels loaded with Anti-miR21 (As-21) suppressed VEGF secretion and the tumor associated angiogenesis.

√ As-21 loaded nanohydrogels provoked apoptosis of tumor cells though ROS generation and caspase 3 activation.

VEGF-induced angiogenesis through the miR-21/VEGF/VEGFR2 signaling pathway [46]. Interestingly, As-21/NG disrupted capillary formation by HUVECs (Fig. 7B and Fig. 7C), possibly due to decreased VEGF secretion (Fig. 7A). Moreover, transfection with As-21 or Scr alone did not influence the tube formation. In line with previous results,[12] VEGF had a promoting role in the formation of new blood vessels on the CAM (Fig. 8), while miR-21 suppression prevented the VEGF stimulatory effect on neovascularization.

Conclusively, As-21/NG, either alone or in combination with chemotherapeutic agents such cis-Pt, is suggested for treating resistant tumor cells to inhibit tumor-associated angiogenesis, though further *in-vitro* and *in-vivo* investigations are warranted.

Conclusion

In the current study, we report the development of PEG5k-CMPEI NG loaded with As-21 in order to sensitize ovarian cells to Cis-Pt. Indeed, it was found that PEG5k-CMPEI NG loaded with As-21 can effectively increase ROS formation, decrease Cas3 activity and inhibit angiogenesis in A2780R and A2780S ovarian cancer cell lines.

Ethical Approval

All procedures performed in this study were in accordance with the ethical standards and animal study guidelines approved by SUMS.

Competing interests

The authors declare there is no conflict of interest.

Authors' contribution

AMT and SSA conceived and planned the experiments, SJ conducted the experiments, analyzed the results, and was responsible for writing

the manuscript, MJM participated in developing the CAM model. All authors reviewed the manuscript and confirmed its submission to the journal.

Supplementary Materials

Supplementary file 1 contains Fig. S1.

References

1. Koushik A, Grundy A, Abrahamowicz M, Arseneau J, Gilbert L, Gotlieb WH, *et al.* Hormonal and reproductive factors and the risk of ovarian cancer. *Cancer Causes Control* **2017**; 28: 393-403. https://doi.org/10.1007/s10552-016-0848-9

2. Andrews PA, Velury S, Mann SC, Howell SB. cis-Diamminedichloroplatinum (II) accumulation in sensitive and resistant human ovarian carcinoma cells. *Cancer Res* **1988**; 48: 68-73.

3. Ikeguchi M, Nakamura S, Kaibara N. Quantitative analysis of expression levels of bax, bcl-2, and survivin in cancer cells during cisplatin treatment. *Oncol Rep* **2002**; 9: 1121-6. https://doi.org/10.3892/or.9.5.1121

4. Ganesh S, Iyer AK, Weiler J, Morrissey DV, Amiji MM. Combination of siRNA-directed gene silencing with cisplatin reverses drug resistance in human non-small cell lung cancer. *Mol Ther Nucleic Acids* **2013**; 2. https://doi.org/10.1038/mtna.2013.29

5. Pillai RS. MicroRNA function: multiple mechanisms for a tiny RNA? *RNA* **2005**; 11: 1753-61. https://doi.org/10.1261/rna.2248605

6. Javanmardi S, Reza Aghamaali M, Sadat Abolmaali S, Mohammadi S, Mohammad Tamaddon A. miR-21, An Oncogenic Target miRNA for Cancer Therapy: Molecular Mechanisms and Recent Advancements in Chemo and Radio-resistance. *Curr Gene Ther* **2016**; 16: 375-89. https://doi.org/10.2174/156652321766617010210 5119

7. Chan JK, Blansit K, Kiet T, Sherman A, Wong G, Earle C, *et al.* The inhibition of miR-21 promotes apoptosis and chemosensitivity in ovarian cancer. *Gynecol Oncol* **2014**; 132: 739-44. https://doi.org/10.1016/j.ygyno.2014.01.034

8. Zhang X, Ng W-L, Wang P, Tian L, Werner E, Wang H, *et al.* MicroRNA-21 modulates the levels of reactive oxygen species by targeting SOD3 and TNFα. *Cancer Res* **2012**. https://doi.org/10.1158/0008-5472.CAN-12-0639

9. Ling M, Li Y, Xu Y, Pang Y, Shen L, Jiang R, *et al.* Regulation of miRNA-21 by reactive oxygen species-activated ERK/NF-κB in arsenite-induced cell transformation. *Free Radic Biol Med* **2012**; 52: 1508-18. https://doi.org/10.1016/j.freeradbiomed.2012.02.020

10. Lou Y, Yang X, Wang F, Cui Z, Huang Y. MicroRNA-21 promotes the cell proliferation, invasion and migration abilities in ovarian epithelial carcinomas through inhibiting the expression of PTEN protein. *Int J Mol Med* **2010**; 26: 819-27. https://doi.org/10.3892/ijmm_00000530

11. Liu S, Fang Y, Shen H, Xu W, Li H. Berberine sensitizes ovarian cancer cells to cisplatin through miR-21/PDCD4 axis. *Acta Biochim Biophys Sin* **2013**; 45: 756-62. https://doi.org/10.1093/abbs/gmt075

12. Echevarría-Vargas IM, Valiyeva F, Vivas-Mejía PE. Upregulation of miR-21 in cisplatin resistant ovarian cancer via JNK-1/c-Jun pathway. *PLoS One* **2014**; 9: e97094. https://doi.org/10.1371/journal.pone.0116447

13. Zou L, Song X, Yi T, Li S, Deng H, Chen X, *et al.* Administration of PLGA nanoparticles carrying shRNA against focal adhesion kinase and CD44 results in enhanced antitumor effects against ovarian cancer. *Cancer Gene Ther* **2013**; 20: 242. https://doi.org/10.1038/cgt.2013.12

14. Polyak D, Krivitsky A, Scomparin A, Eliyahu S, Kalinski H, Avkin-Nachum S, *et al.* Systemic delivery of siRNA by aminated poly (α) glutamate for the treatment of solid tumors. *J Control Release* **2017**; 257: 132-43. https://doi.org/10.1016/j.jconrel.2016.06.034

15. Yin H, Kanasty RL, Eltoukhy AA, Vegas AJ, Dorkin JR, Anderson DG. Non-viral vectors for gene-based therapy. *Nat Rev Genet* **2014**; 15: 541. https://doi.org/10.1038/nrg3763

16. Baker A, Saltik M, Lehrmann H, Killisch I, Mautner V, Lamm G, *et al.* Polyethylenimine (PEI) is a simple, inexpensive and effective reagent for condensing and linking plasmid DNA to adenovirus for gene delivery. *Gene Ther* **1997**; 4: 773. https://doi.org/10.1038/sj.gt.3300471

17. Javanmardi S, Tamaddon AM, Aghamaali MR, Ghahramani L, Abolmaali SS. Redox-sensitive, PEG-shielded carboxymethyl PEI nanogels silencing MicroRNA-21, sensitizes resistant ovarian cancer cells to cisplatin. *Asian J Pharm Sci* **2018**. https://doi.org/10.1016/j.ajps.2018.10.006

18. Abolmaali SS, Tamaddon AM, Dinarvand R. Nano-hydrogels of methoxy polyethylene glycol-grafted branched polyethyleneimine via biodegradable cross-linking of Zn 2+-ionomer micelle template. *J Nanopart Res* **2013**; 15: 2134. https://doi.org/10.1007/s11051-013-2134-z

19. Pozzi D, Colapicchioni V, Caracciolo G, Piovesana S, Capriotti AL, Palchetti S, *et al.* Effect of polyethyleneglycol (PEG) chain length on the bio–nano-interactions between PEGylated lipid nanoparticles and biological fluids: from nanostructure to uptake in cancer cells. *Nanoscale* **2014**; 6: 2782-92. https://doi.org/10.1039/c3nr05559k

20. Stocks SJ, Jones AJ, Ramey CW, Brooks DE. A fluorometric assay of the degree of modification of protein primary amines with polyethylene glycol. *Anal Biochem* **1986**; 154: 232-4. https://doi.org/10.1016/0003-2697(86)90520-8

21. Freedman R, Radda G. The reaction of 2, 4, 6-trinitrobenzenesulphonic acid with amino acids, peptides and proteins. *Biochem J* **1968**; 108: 383-91. https://doi.org/10.1042/bj1080383

22. Bir K, Crawhall JC, Mauldin D. Reduction of disulfides with sodium and potassium borohydrides and its application to urinary disulfides. *Clin Chim Acta* **1970**; 30: 183-90. https://doi.org/10.1016/0009-8981(70)90207-X

23. Najafi H, Abolmaali SS, Owrangi B, Ghasemi Y, Tamaddon AM. Serum resistant and enhanced transfection of plasmid DNA by PEG-stabilized polyplex nanoparticles of L-histidine substituted polyethyleneimine. *Macromol Res* **2015**; 23: 618-27. https://doi.org/10.1007/s13233-015-3074-5

24. Yu X, Chen Y, Tian R, Li J, Li H, Lv T, *et al.* miRNA-21 enhances chemoresistance to cisplatin in epithelial ovarian cancer by negatively regulating PTEN. *Oncol Lett* **2017**; 14: 1807-10. https://doi.org/10.3892/ol.2017.6324

25. Dong C, Liu X, Wang H, Li J, Dai L, Li J, *et al.* Hypoxic non-small-cell lung cancer cell-derived exosomal miR-21 promotes resistance of normoxic cell to cisplatin. *Onco Targets Ther* **2019**; 12: 1947. https://doi.org/10.2147/OTT.S186922

26. Roeckl W, Hecht D, Sztajer H, Waltenberger J, Yayon A, Weich HA. Differential binding characteristics and cellular inhibition by soluble VEGF receptors 1 and 2. *Exp Cell Res* **1998**; 241: 161-70. https://doi.org/10.1006/excr.1998.4039

27. Arnaoutova I, Kleinman HK. In vitro angiogenesis: endothelial cell tube formation on gelled basement membrane extract. *Nat. Protoc.* **2010**; 5: 628. https://doi.org/10.1038/nprot.2010.6

28. Norrby K. In vivo models of angiogenesis. *J Cell Mol Med* **2006**; 10: 588-612. https://doi.org/10.1111/j.1582-4934.2006.tb00423.x

29. Mawhinney DB, Yates Jr JT. FTIR study of the oxidation of amorphous carbon by ozone at 300 K—Direct COOH formation. *Carbon* **2001**; 39: 1167-73. https://doi.org/10.1016/S0008-6223(00)00238-4

30. Scott V, Clark AR, Docherty K. The Gel Retardation Assay. In: Harwood AJ, editor. *Protocols for Gene Analysis*. Totowa, NJ: Humana Press; **1994**. p. 339-47. https://doi.org/10.1385/0-89603-258-2:339

31. Kleemann E, Neu M, Jekel N, Fink L, Schmehl T, Gessler T, *et al.* Nano-carriers for DNA delivery to the lung based upon a TAT-derived peptide covalently coupled to PEG–PEI. *J Control Release* **2005**; 109: 299-316. https://doi.org/10.1016/j.jconrel.2005.09.036

32. Santos JL, Pandita D, Rodrigues J, Pêgo AP, Granja PL, Balian G, *et al.* Receptor-mediated gene delivery using PAMAM dendrimers conjugated with peptides recognized by mesenchymal stem cells. *Mol Pharm* **2010**; 7: 763-74. https://doi.org/10.1021/mp9002877

33. Dehshahri A, Oskuee RK, Shier WT, Hatefi A, Ramezani M. Gene transfer efficiency of high primary amine content,

hydrophobic, alkyl-oligoamine derivatives of polyethylenimine. *Biomaterials* **2009**; 30: 4187-94. https://doi.org/10.1016/j.biomaterials.2009.04.036

34. Cheng W, Yang C, Hedrick JL, Williams DF, Yang YY, Ashton-Rickardt PG. Delivery of a granzyme B inhibitor gene using carbamate-mannose modified PEI protects against cytotoxic lymphocyte killing. *Biomaterials* **2013**; 34: 3697-705. https://doi.org/10.1016/j.biomaterials.2013.01.090

35. Abolmaali SS, Tamaddon AM, Mohammadi S, Amoozgar Z, Dinarvand R. Chemically crosslinked nanogels of PEGylated poly ethyleneimine (l-histidine substituted) synthesized via metal ion coordinated self-assembly for delivery of methotrexate: cytocompatibility, cellular delivery and antitumor activity in resistant cells. *Mater Sci Eng C* **2016**; 62: 897-907. https://doi.org/10.1016/j.msec.2016.02.045

36. Verbaan F, Oussoren C, Van Dam I, Takakura Y, Hashida M, Crommelin D, *et al.* The fate of poly (2-dimethyl amino ethyl) methacrylate-based polyplexes after intravenous administration. *Int J Pharm* **2001**; 214: 99-101. https://doi.org/10.1016/S0378-5173(00)00642-6

37. Golkar N, Samani SM, Tamaddon AM. Cholesterol-conjugated supramolecular assemblies of low generations polyamidoamine dendrimers for enhanced EGFP plasmid DNA transfection. *J Nanopart Res* **2016**; 18: 107. https://doi.org/10.1007/s11051-016-3413-2

38. Malik N, Wiwattanapatapee R, Klopsch R, Lorenz K, Frey H, Weener JW, *et al.* Dendrimers: relationship between structure and biocompatibility in vitro, and preliminary studies on the biodistribution of 125I-labelled polyamidoamine dendrimers in vivo. *J Control Release* **2000**; 65: 133-48. https://doi.org/10.1016/S0168-3659(99)00246-1Get

39. Venault A, Huang Y-C, Lo J, Chou C-J, Chinnathambi A, Higuchi A, *et al.* Tunable PEGylation of branch-type PEI/DNA polyplexes with a compromise of low cytotoxicity and high transgene expression: in vitro and in vivo gene delivery. *J Mater Chem B* **2017**; 5: 4732-44. https://doi.org/10.1039/C7TB01046J

40. Soshilov AA, Denison MS. DNA binding (gel retardation assay) analysis for identification of aryl hydrocarbon (Ah) receptor agonists and antagonists. *Optimization in Drug Discovery: In Vitro Methods* **2014**; 207-19. DOI: 10.1007/978-1-62703-742-6_12

41. Zheng N, Song Z, Liu Y, Zhang R, Zhang R, Yao C, *et al.* Redox-responsive, reversibly-crosslinked thiolated cationic helical polypeptides for efficient siRNA encapsulation and delivery. *J Controlled Release* **2015**; 205: 231-9. https://doi.org/10.1016/j.jconrel.2015.02.014

42. Foged C, Brodin B, Frokjaer S, Sundblad A. Particle size and surface charge affect particle uptake by human dendritic cells in an in vitro model. *Int J Pharm* **2005**; 298: 315-22. https://doi.org/10.1016/j.ijpharm.2005.03.035

43. Juan MEl, Wenzel U, Daniel H, Planas JM. Resveratrol induces apoptosis through ROS-dependent mitochondria pathway in HT-29 human colorectal carcinoma cells. *J Agr Food Chem* **2008**; 56: 4813-8. https://doi.org/10.1021/jf800175a

44. Liu L-Z, Li C, Chen Q, Jing Y, Carpenter R, Jiang Y, *et al.* MiR-21 induced angiogenesis through AKT and ERK activation and HIF-1α expression. *PloS One* **2011**; 6: e19139. https://doi.org/10.1371/journal.pone.0019139

45. Liu Y, Luo F, Wang B, Li H, Xu Y, Liu X, *et al.* STAT3-regulated exosomal miR-21 promotes angiogenesis and is involved in neoplastic processes of transformed human bronchial epithelial cells. *Cancer Lett* **2016**; 370: 125-35. https://doi.org/10.1016/j.canlet.2015.10.011

46. Sun X, Ma X, Wang J, Zhao Y, Wang Y, Bihl JC, *et al.* Glioma stem cells-derived exosomes promote the angiogenic ability of endothelial cells through miR-21/VEGF signal. *Oncotarget* **2017**; 8: 36137. https://doi.org/10.1016/j.canlet.2015.10.011